34th Annual International Conference of the IEEE EMBS
San Diego, California USA, 28 August - 1 September, 2012

Can electric current steering be used to control perception of a retinal prosthesis patient?*

Craig O. Savage[♡,1,2] Filiz Isabell Kiral-Kornek[1,2] Bahman Tahayori[1,2] David B. Grayden[1,2,3,4]

Abstract— **We consider a form of current steering to elicit desired perceptions in users of a retinal prosthesis. While it is common to use a single, remote return electrode to balance electrical stimulation, advances in chip design and electrical switching have enabled more flexibility in stimulation paradigms. We have created a finite-element model of a retina and a ten electrode prosthesis in COMSOL. Different configurations of stimulating and return electrodes are considered and employed to predict possible user perception. We investigate charge balance on electrodes in our varying geometries and consider the impact of inhomogeneous resistance between electrodes and the tissue.**

I. Introduction

Retinal implants have been shown to provide visual input to blind patients via electrical stimulation [6], [14]. Electrical stimulation of the retina results in perceived dots of light known as "phosphenes". These phosphenes have been described as circles or ovals, or as a bright centre and dark surrounding ring [5], [6]. They have been reported as predominantly yellow or white, with red-orange or black occasionally occurring, and blue after cessation of high-frequency stimulation [6]. This model of a single phosphene per electrical stimulation has led to simulated phosphenated vision, which has been used for algorithm development as a model of the types of information that can be presented to a user of a retinal implant [1], [8], [11]. Such phosphenes have been described as being brighter with increasing current amplitude, stimulation duration, interphase gap between stimulation phases, and frequency of stimulation [3], [5], [6], [10]. It has been reported that larger current amplitudes also result in larger percepts [6].

If multiple electrodes are stimulated, retinal implantees are able to distinguish different spatiotemporal characteristics of stimulation. Perceptual differences include simultaneous versus sequential stimulation, and clockwise versus counter-clockwise stimulation of groups of electrodes [4]. It has been theorised that such differences are consistent with interference patterns of electric fields [4].

*This research was supported by the Australian Research Council (ARC) through its Special Research Initiative (SRI) in Bionic Vision Science and Technology grant to Bionic Vision Australia (BVA).

[1] NeuroEngineering Laboratory, Dept. of Electrical and Electronic Engineering, University of Melbourne, VIC 3010 Australia

[2] Centre for Neural Engineering, University of Melbourne, VIC 3010 Australia.

[3] NICTA Victoria Research Labs, The University of Melbourne, VIC 3010 Australia

[4] Bionics Institute, 384-388 Albert St, East Melbourne, VIC 3002 Australia

[♡] Correspondence to be sent to: cosavage@unimelb.edu.au

In simulation, it has also been shown that the geometry between stimulating and return electrodes creates variation in the electric field around electrodes [13]. This effect, termed "crosstalk", could then create different perceptions to a retinal implant user. Assuming that crosstalk results in different perceptions, it can be used to present various phosphene shapes to an implantee which may result in a more effective visual perception. We investigate the effect of different selections of stimulating and return electrodes on charge density and use charge density as a predictor of patient perception. Example applications of different perceptions are covered in another work [7].

If such a strategy were to be used in a chronic manner, it would need to be safe and efficacious. One concern for safe chronic stimulation is charge balance; chronic charge imbalances may result in corrosion of electrodes and tissue damage [9]. While previous works focus on charge balance on the stimulating electrode, here we consider whether charge is balanced on stimulating and return electrodes. Furthermore, we consider charge balance in an environment in which the resistance between the electrodes and tissue is not constant. We consider the evolution of residual current density to estimate charge imbalance, if any, on electrodes.

We follow the general procedure of a previous study [13], in which the electric field distribution is modelled in COMSOL. In contrast to that work [13], we consider a rectangular grid of electrodes rather than a hexagonal grid. We perform simulations of the current density for different combinations of stimulating and return electrodes, as well as homogeneous and inhomogeneous resistances.

The remainder of the paper is organised as follows. In Section II, we outline the procedure of modelling implantee perception as a function of the electric field. Section III contains plots of our results, including predictions as to patient perception, and an evaluation of charge balance on electrodes. Finally, in Section IV, we discuss some of the potential implications of our results, and consider potential extensions of our work.

II. Methods

Different electrode configurations are simulated in the finite element simulation tool COMSOL 4.2a. In simulating the current density around electrodes, the "Electric Current (ec)" model in the AC/DC module is selected. In order to follow the behaviour of the current density around electrodes in time, the "Time Dependent" study type is selected to solve the relevant partial differential equations. In all simulations, COMSOL internal analytic functions are

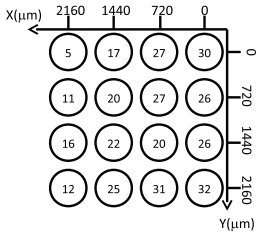

Fig. 1. Variation in electrode impedance from a characterised 4×4 grid of electrodes. The diagram shows the electrode geometry, with an estimated resistance values in kΩ on each electrode, as detailed elsewhere [6].

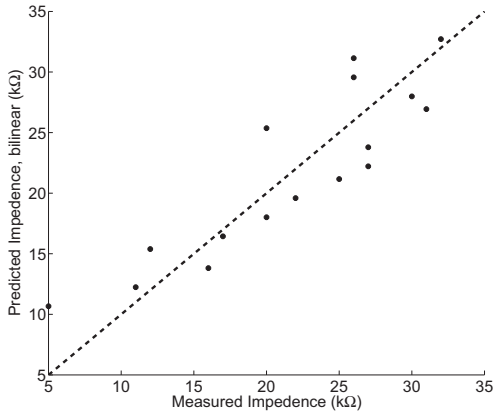

Fig. 2. Comparison of observed impedance values for the electrode data as shown in Figure 1, compared to model predictions from (1).

employed to define the desired waveform for each electrode. The solver we have selected is "Direct MUMPS" (with its default parameters) to find the current density map as a result of electrode activations. In each model, a stimulating electrode is surrounded by eight electrodes that are either floating or at ground potential. For evaluation of the results, we display the current density in Section III.

We investigated the following cases:

1) A single distant, common return electrode. This was selected as a control and was the configuration used in prior literature [3], [4], [6]. In our simulations, this common return was located $1.6\mathrm{mm}$ from the stimulating electrode, or over $6\times$ the distance between stimulating and return electrodes.
2) The surrounding 8 electrodes serving as return (or "guard") electrodes. This was chosen to compare to the hexagonal return configuration of a similar work [13].
3) The middle left and right electrodes serving as return.
4) The middle top and bottom electrodes serving as return.
5) The diagonal electrodes (i.e., upper left–lower right, and upper right–lower left) serving as return.
6) Four electrodes in an unbalanced manner, with the top row and central bottom (i.e., a "T") serving as return.
7) Four surrounding electrodes serving as return. These were arranged in a diagonal (i.e., in the shape of an "X"), or central (i.e., in the shape of a "+") manner.

In each of the above, we employed a stimulation waveform with a cathodic phase first, no interphase gap, and an equal anodic phase. Each phase duration was $500\mu\mathrm{s}$ with a normalised current amplitude, as we are only concerned about relative values of current density.

We assume a linearly varying resistance over the grid in horizontal and vertical directions. These slowly changing resistance values approximate the change in average observed impedance for a 4×4 grid of electrodes in a retinal implant [6]. An illustration of electrode impedance used to generate our impedance variation is shown in Figure 1.

From the data in Figure 1, an affine function in two dimensions was used to model the impedance at an arbitrary electrode. The resulting equation was:

$$Z = 28 - 0.80x/100 + 0.22y/100 \qquad (1)$$

where Z is the resistance in $\mathrm{k}\Omega$, and x and y are distances in $\mu\mathrm{m}$. A comparison of the fit of the prediction and observed impedance are shown in Figure 2. The linear model is a good predictor of observed impedence, and has an R^2 value of 0.78.

III. Results

We aim to show that return electrode geometry changes the current density, thereby changing patient perception. We further hypothesize that charge is balanced on return electrodes, in both uniform and varying impedances between electrodes and tissue. Charge balance is shown by a decay of current density after stimulation.

In Figure 3, we present the main set of results of this work; namely, we overlay the current density at the end of the first phase of stimulation (i.e., at $t = 0.99\mathrm{ms}$), and use this as a predictor of patient perception. For example, in Figure 3(c), we demonstrate that current density can be shifted to be horizontal. We infer this would produce an elliptical phosphene oriented with the major axis horizontal. Conversely, in Figure 3(d), our selection of return electrodes produces a current density aligned in the vertical direction which we model as producing an ellipse that has its major axis orthogonal to the one in Figure 3(c).

We also considered whether or not having multiple returns would be safe, from the point of view of charge balance. In symmetric cases, one could argue that the charge in and out would be the same; however, our model has inhomogeneous impedance. To this end, we considered the magnitude of the current density over our grid of electrodes at the end of stimulation (i.e., $1.01\mathrm{ms}$). In each case, the residual current density was less than $10^{-6}\mu\mathrm{A/cm}^2$, and decreased as time progressed. The stimulation with the largest residual current density was the common return. Illustrations of the decay of residual current density following stimulation are shown in Figure 4.

Note that the scale of residual current density decays quickly after the cessation of stimulation. At the end of stimulation, maximal current densities are on the

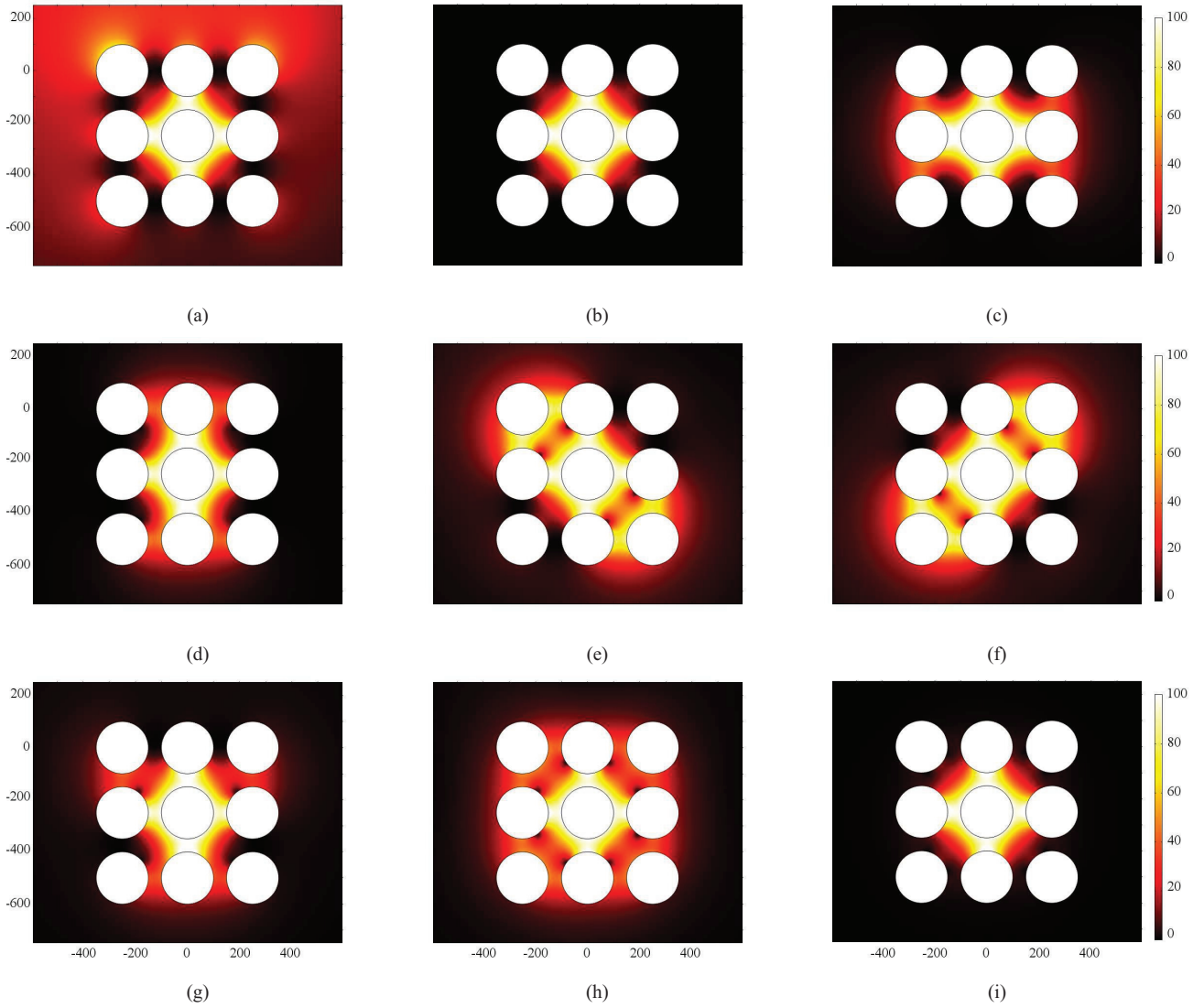

Fig. 3. Different patterns of return electrodes. In each case, the stimulating electrode is the centre electrode, and the returns are connected to ground potential. The plots are near the end of the second phase of the stimulation pulse (0.99ms). The return electrodes are selected as: (a) Distant return, (b) All 8 surrounding electrodes, (c) Horizontally, (d) Vertically, (e) Upper-left to lower-right, (f) Upper-right to lower-left, (g) A "T", (h) An "X", (i) A "+".

order of $100\mu\mathrm{A/cm}^2$, and this drops to the order of $10^{-6}\mu\mathrm{A/cm}^2$ after stimulation and quickly decays to near zero ($10^{-20}\mu\mathrm{A/cm}^2$) in the vicinity of the simulated region.

IV. Discussion

We have presented results demonstrating the impact of different return electrode geometries on current density. The immediate question is whether current density is an appropriate proxy for patient perception, as we have not modelled nor considered the biological elements responsible for perception.

Our results generally agree with a previous study on crosstalk [13], in that a distant common return creates larger current spreads, whereas multiple surrounds produces a more localised result. The results in Figure 3 show little difference between the 8 electrode surround return and the "+" return structure, but there is a difference in the "X" method. Hence, we conclude that the geometry of return electrodes, in addition to their number, influences current spread and, therefore, may play an important role in patient perception.

We have further considered variable impedance in this work, assuming an affine impedance map that approximates electrode results from the literature [6]. However, the length scale of that study is different from ours, and it is unclear whether the difference in our electrode size and relative distance plays a large role. Subsequent studies found that smaller electrodes had larger impedances [2], and we have not modified the impedance values to match our study.

Finally, our results indicate that residual current density is minimal for different allocation of return electrodes, and we predict that different combinations of return electrodes provide less residual than a common return.

In the future, we intend to conduct experiments with a multi-channel stimulator [12] to verify these results, in terms of the electrical predictions of current density and charge balance. Assuming we confirm our simulations, we then aim

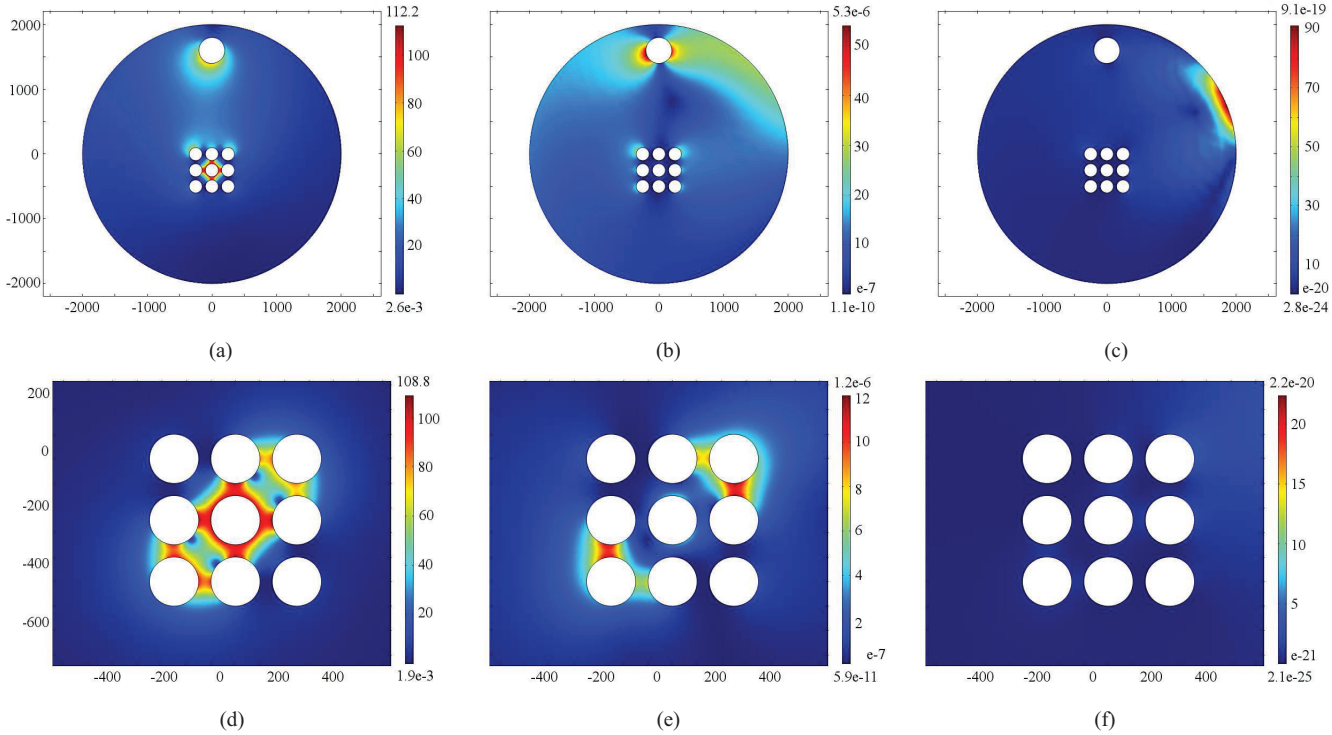

Fig. 4. Decay of residual current density, in $\mu\mathrm{A/cm}^2$, following stimulation for a common return (top, (a) - (c)) and diagonal return electrodes (bottom, (d)-(f)). The plots increase in time from left to right, and represent the end of stimulation, with $t = 0.99\mathrm{ms}$ ((a), (d)), just after stimulation $t = 1.01\mathrm{ms}$ ((b),(e)), and residual current densities after stimulation $t = 1.03\mathrm{ms}$ ((c),(f)).

to test these methods *in vitro* and *in vivo* to verify that current density is a predictor of retinal ganglion cell spike rate and evoked cortical responses.

Acknowledgments

This research was supported by the Australian Research Council (ARC) through its Special Research Initiative (SRI) in Bionic Vision Science and Technology grant to Bionic Vision Australia (BVA). The Bionics Institute acknowledges the support it receives from the Victorian Government through its Operational Infrastructure Support Program.

References

[1] S. Chen, G. Suaning, J. Morley, and N. Lovell, "Simulating prosthetic vision: I. Visual models of phosphenes," pp. 1493–1506, 2009.

[2] C. de Balthasar, S. Patel, A. Roy, R. Freda, S. Greenwald, A. Horsager, M. Mahadevappa, D. Yanai, M. McMahon, M. Humayun, R. Greenberg, J. Weiland, and I. Fine, "Factors affecting perceptual thresholds in epiretinal prostheses," *Investigative Ophtalmology & Visual Science*, vol. 49, no. 6, pp. 2303–2314, 2008.

[3] S. Greenwald, A. Horsager, M. Humayun, R. Greenberg, M. McMahon, and I. Fine, "Brightness as a function of current amplitude in human retinal electrical stimulation," *Investigative Ophthalmology & Visual Science*, vol. 50, no. 11, pp. 5017–5025, 2009.

[4] A. Horsager, R. Greenberg, and I. Fine, "Spatiotemporal interactions in retinal prosthesis subjects," *Investigative Ophthalmology & Visual Science*, vol. 51, no. 2, pp. 1223–1233, 2010.

[5] A. Horsager, S. Greenwald, J. Weiland, M. Humayun, R. Greenberg, M. McMahon, G. Boynton, and I. Fine, "Predicting visual sensitivity in retinal prosthesis patients," *Investigative Ophthalmology & Visual Science*, vol. 50, no. 4, pp. 1483–1491, 2009.

[6] M. Humayun, J. Weiland, G. Fujii *et al.*, "Visual perception in a blind subject with a chronic microelectronic retinal prosthesis," *Vision Research*, vol. 43, no. 24, pp. 2573–2581, 2003.

[7] F. I. Kiral Kornek, C. O. Savage, and D. B. Grayden, "Feature accentuation in phosphenized images," in *Submitted to the 34th Annual International Conference of the IEEE Engineering in Medicine & Biology Society (EMBC)*, 2012.

[8] P. Lieby, N. Barnes, C. McCarthy, N. Liu, H. Dennett, J. G. Walker, and V. Botea, "Substituting depth for intensity and real-time phosphene rendering: Visual navigation under low vision conditions," in *Proceedings of the 33rd Annual Engineering in Medicine and Biology Conference (EMBC)*, 2011, pp. 8017–8020.

[9] D. Merrill, M. Bikson, and J. Jefferys, "Electrical stimulation of excitable tissue: Design of efficacious and safe protocols," *Journal of Neuroscience Methods*, vol. 141, no. 2, pp. 171–198, 2004.

[10] C. O. Savage, D. B. Grayden, H. Meffin, and A. N. Burkitt, "Predicting phosphene elicitation in patients with retinal implants: A mathematical study," in *33rd Annual Engineering in Medicine and Biology Conference (EMBC)*, 2011, pp. 6246–9.

[11] A. Stacey, Y. Li, and N. Barnes, "A salient information processing system for bionic eye with application to obstacle avoidance," in *Proceedings of the 33rd Annual Engineering in Medicine and Biology Conference (EMBC)*, 2011, pp. 5116–5119.

[12] N. Tran, S. Skafidas, J. Yang, S. Bai, M. Fu, D. Ng, M. Halpern, and I. Mareels, "A prototype 64-electrode stimulator in 65nm CMOS process towards a high density epi-retinal prosthesis," in *Proceedings of the 33rd Annual Engineering in Medicine and Biology Conference (EMBC)*, 2011, pp. 6729–32.

[13] R. G. H. Wilke, G. K. Moghadam, N. H. Lovell, G. J. Suanning, and S. Dokos, "Electric crosstalk impairs spatial resolution of multi-electrode arrays in retinal implants," *Journal of Neural Engineering*, vol. 8, no. 4, p. 04616, 2011.

[14] E. Zrenner, R. Wilke, K. Bartz-Schmidt, H. Benav, D. Besch, F. Gekeler, J. Koch, K. Porubsk, H. Sachs, and B. Wilhelm, "Blind retinitis pigmentosa patients can read letters and recognize the direction of fine stripe patterns with subretinal electronic implants," vol. 50, pp. E–Abstract 4581, 2009.